Incoherent noise suppression with curvelet-domain sparsity

Vishal Kumar, EOS-UBC and Felix J. Herrmann, EOS-UBC*

SUMMARY

The separation of signal and noise is a key issue in seismic data processing. By noise we refer to the incoherent noise that is present in the data. We use the recently introduced multiscale and multidirectional curvelet transform for suppression of random noise. The curvelet transform decomposes data into directional plane waves that are local in nature. The coherent features of the data occupy the large coefficients in the curvelet domain, whereas the incoherent noise lives in the small coefficients. In other words, signal and noise have minimal overlap in the curvelet domain. This gives us a chance to use curvelets to suppress the noise.

INTRODUCTION

In seismic data, recorded wave fronts (i.e. reflections), arise from the interaction of the incident wave field with inhomogeneities in the Earth's subsurface. The wave fronts can get contaminated with noise during aquisition or even due to processing problems. The forward problem of seismic denoising can be written as:

$$\mathbf{y} = \mathbf{m} + \mathbf{n}, \tag{1}$$

where $\mathbf{y}$ is the known noisy data, $\mathbf{m}$ is the unknown model (noise-free data) and $\mathbf{n}$ is the noise. Our objective is to recover $\mathbf{m}$. As seismic data are contaminated with random noise, many methods have been developed to suppress such incoherent noise. Some of these techniques discriminate between signal and noise based on their frequency content (bandpass filter) or they use some sort of prediction filter (F-X Deconvolution). Such methods do remove the random noise but at the same time they may remove some of the signal energy (Neelamani et al., 2008). More recently, wavelet transform based processing has been applied for noise suppression. The wavelet transform is good for point-like events (one-dimensional singularity). However, for higher dimensions (e.g seismic data), wavelets fail to give a parsimonious representation. In this work, we use the recently introduced curvelet transform to suppress random noise. The signal and noise have minimal overlap in the curvelet domain (Neelamani et al., 2008). This makes the curvelet transform the ideal choice for detecting wave fronts and suppressing noise. For this work, we cast the denoising problem as an inverse problem. We compare this method with hard thresholding and soft thresholding of curvelet coefficients for a fixed threshold. We start with a brief introduction to curvelets, followed by a presentation of our algorithm and application to synthetic data.

CURVELETS

Curvelets are amongst one of the latest members of the family of multiscale and multidirectional transforms (Candés et al., 2006). They are tight frames (energy preserving transform) with moderate redundancy. A curvelet is strictly localized in frequency and pseudo-localized in space; i.e., it has a rapid spatial decay. In the physical domain, curvelets look like little plane waves that are oscillatory in one direction and smooth in perpendicular directions. In the F-K domain each curvelet lives in an angular wedge. Each curvelet is associated with a position, frequency bandwidth and an angle. Different curvelets at different frequencies, angles and positions are shown in Fig. 1. The construction of curvelets is such that any object with wavefront-like structure (e.g seismic images) can be represented by relatively few significant transform coefficients (Candés et al., 2006). Hence, these objects are sparse in the curvelet domain and we would enforce the sparsity of seismic data while solving the inverse problem.

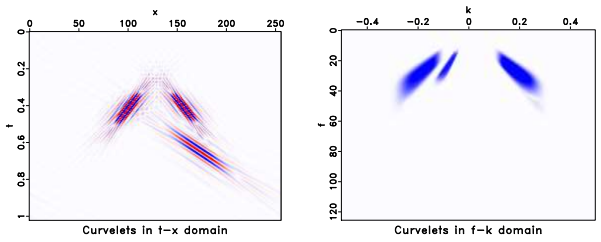

(a) (b)

Figure 1: A few curvelets in both t-x (left) and F-K domain (right).

METHOD

The model $\mathbf{m}$ from the forward problem (Eq. 1) can be expanded in terms of curvelet coefficients. Eq. 1 is now modified as:

$$\mathbf{y} = \mathbf{C^T x} + \mathbf{n}, \tag{2}$$

where $\mathbf{x}$ is the curvelet transform vector and $\mathbf{C^T}$ is the curvelet transform synthesis operator. The denoising problem with curvelet-domain sparsity can be cast into the following constrained optimization problem (Elad et al., 2005):

$$\mathbf{P}_\varepsilon : \quad \begin{cases} \tilde{\mathbf{x}} = \arg\min_{\mathbf{x}} ||\mathbf{x}||_1 \quad \text{s.t.} \quad ||\mathbf{y} - \mathbf{C^T x}||_2 \leq \varepsilon, \\ \tilde{\mathbf{m}} = \mathbf{C^T}\tilde{\mathbf{x}}, \end{cases} \tag{3}$$

where $\tilde{\mathbf{x}}$ represents the estimated curvelet transform coefficient vector, $\tilde{\mathbf{m}}$ is the estimated model and ε is proportional to the noise level. By solving Eq. 3, we try to find the sparsest set of curvelet coefficients (by minimizing the one-norm) which explains the data within the noise level (Hennenfent et al., 2005). In our case, the above constrained optimization problem (Eq. 3) is solved by a series of the following unconstrained optimization problems (Herrmann and Hennenfent, 2008):

$$\tilde{\mathbf{x}} = \arg\min_{\mathbf{x}} \frac{1}{2}||\mathbf{y} - \mathbf{C^T x}||_2^2 + \lambda ||\mathbf{x}||_1, \tag{4}$$

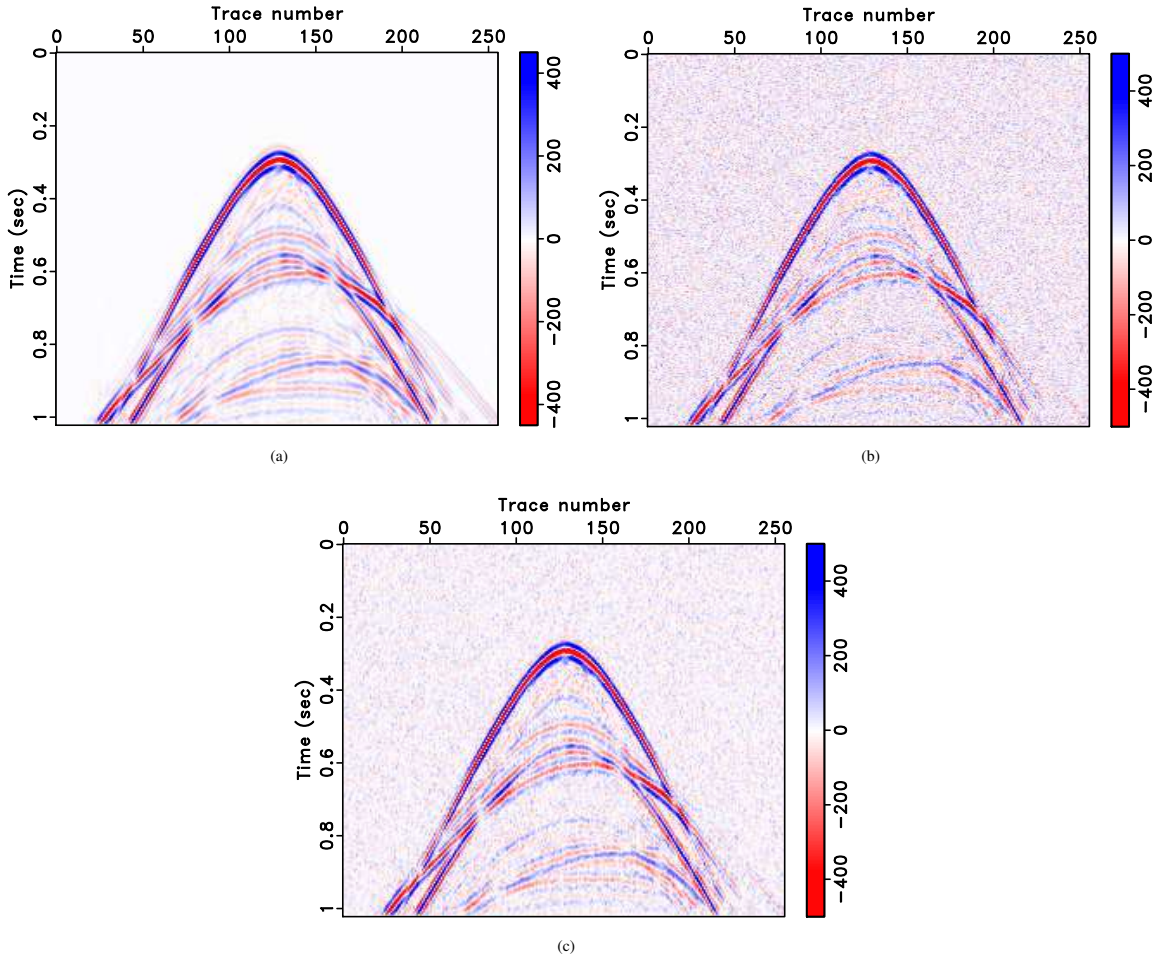

Figure 2: Prestack (a) noise-free data (model), noisy data with (b) white noise (c) colored noise

where λ is the regularization parameter that determines the trade-off between data consistency and the sparsity in the curvelet domain. Eq. 4 is solved by iterative soft thresholding (Daubechies et al., 2004). The solution is found by updating $\mathbf{x}$ as:

$$\mathbf{T}_\lambda : \quad \begin{cases} \mathbf{x} \leftarrow \mathbf{S}_\lambda(\mathbf{x} + \mathbf{C}(\mathbf{y} - \mathbf{C}^{\mathbf{T}}\mathbf{x})), \text{ where} \\ \mathbf{S}_\lambda(x) = sgn(x) \cdot \max(0, |x| - |\lambda|), \end{cases} \tag{5}$$

where $\mathbf{S}_\lambda$ is the soft thresholding operator. We solve a series of such problems (Eq. 4) starting with high λ and decreasing the value of λ until $||\mathbf{y} - \mathbf{C}^{\mathbf{T}}\mathbf{x}||_2 \approx \varepsilon$, which corresponds to the solution of our optimization problem (Lustig et al., 2007). In the case of additive white Gaussian noise with standard deviation σ, the square norm of error $||\mathbf{n}||_2^2$ is a chi-square random variable with mean $\sigma^2 N$ and standard deviation $\sigma^2\sqrt{2N}$, where N is the total number of data points (Candés et al., 2005). For this work, we assume that the probability of $||\mathbf{n}||_2^2$ exceeding its mean plus two standard deviations is small. The maximum $||\mathbf{n}||_2^2$ within two standard deviations is given by $\sigma^2(N + 2\sqrt{2N})$. Thus using an approximate estimate of σ, we solve Eq. 3 with $\varepsilon^2 = \sigma^2(N + 2\sqrt{2N})$.

RESULTS

A synthetic prestack model is used for our experiments. The model (Fig. 2(a)) lives in the frequency range 5-60 Hz. Noisy data (Fig. 2(b)) is obtained by addition of random Gaussian noise (σ=50) to the model. We also created a colored noise realization by doing a band-pass filter (5-60 Hz) on the same white noise. Fig. 2(c) shows the noisy data for additive colored noise. We apply the ℓ_1-norm denoising algorithm to the noisy data to suppress noise. For comparison, we also do hard thresholding of curvelet coefficients, by selecting the coefficients which survive the threshold λ given as:

$$\mathbf{H}_\lambda : \quad \begin{cases} \tilde{\mathbf{m}} = \mathbf{C}^{\mathbf{T}}\mathbf{H}_\lambda(\mathbf{C}\mathbf{y}), \text{ where} \\ \mathbf{H}_\lambda(x) = \mathbf{x}, \text{ if } \mathbf{x} \geq \lambda \\ \mathbf{H}_\lambda(x) = 0, \text{ otherwise} \end{cases} \tag{6}$$

where λ is the threshold level, $\mathbf{H}_\lambda$ is the hard thresholding operator, $\mathbf{C}$ is the forward curvelet transform operator and $\mathbf{C}^{\mathbf{T}}$ is the inverse (adjoint) curvelet transform operator. We also do soft thresholding of curvelet coefficients by selecting the coefficients which survive the threshold λ as defined by $\mathbf{S}_\lambda(x)$ in Eq. 5. The real curvelet transform is used with 5 scales, 16

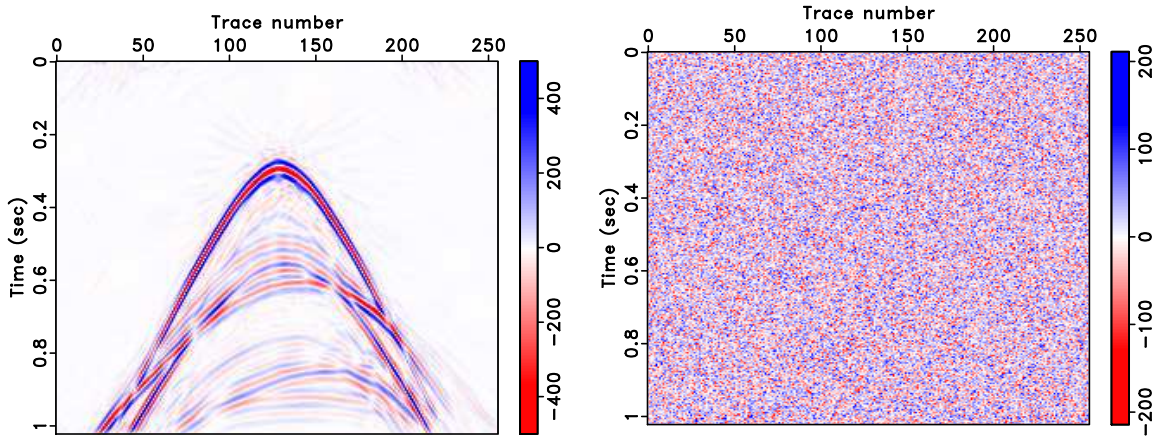

(a) (b)

Figure 3: Prestack data corrupted with white noise: (a) one-norm denoised, (b) difference.

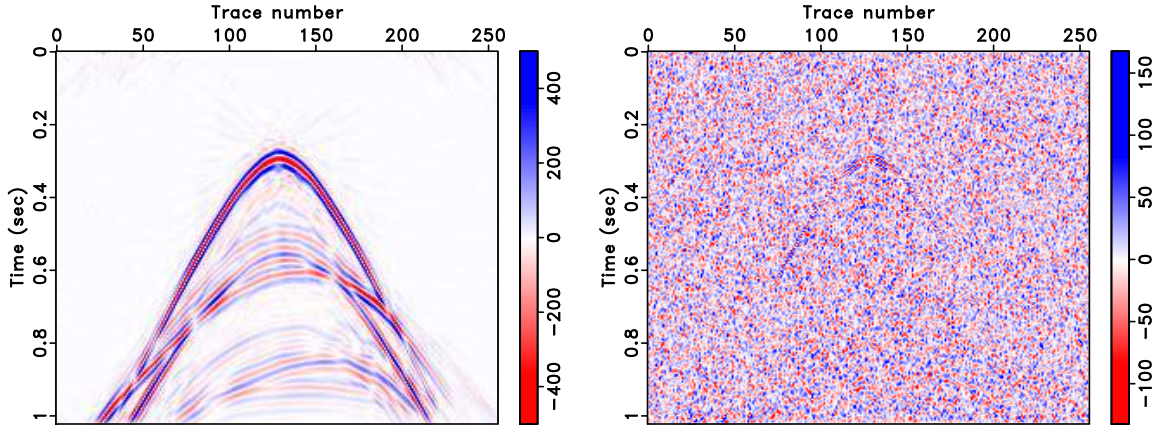

(a) (b)

Figure 4: Prestack data corrupted with colored noise: (a) one-norm denoised, (b) difference.

angles at the 2nd coarsest level and curvelets at the fine scale. For fair comparison, we keep the same ε (noise level estimate or the difference norm) for all three aproaches. All methods are implemented in MATLAB. The signal-to-noise ratio (SNR) is calculated by the following formula:

$$\text{SNR} = 20 * \log_{10} \frac{||model_{actual}||}{||model_{actual} - model_{estimated}||}. \quad (7)$$

For one-norm denoising, the estimated model and the difference is shown in Figs. 3 & 4. The difference for white noise (Fig. 3(b)) has almost no coherent energy while the difference for colored noise (Fig. 4(b)) has some coherent energy present. In terms of the difference, both one-norm (Figs. 3(b) & 4(b)) and hard thresholding (Figs. 5(a) & 6(a)) show that they have minimal impact on the signal energy. The difference image of soft thresholding (Figs. 5(b) & 6(b)) shows a significant amount of coherent energy present. In terms of SNR (Table 1), one-norm denoising (inversion approach) has the highest SNR compared to hard and soft thresholding of curvelet coefficients.

Table 1: SNR comparison for prestack denoising

Noise	Data	One-norm	Hard	Soft
White	3.4403	14.5512	14.2701	12.1783
Color	7.6735	14.7796	14.4846	12.2709

CONCLUSIONS

In this paper, we showed how the ability of curvelets to detect wavefront can be used to suppress incoherent noise. The inversion approach (one-norm denoising) with curvelet-domain sparsity not only recovers the frequency components that are degraded by noise, but also gives the highest SNR for both white and colored noise. Our inversion approach also has minimal impact on the signal energy.

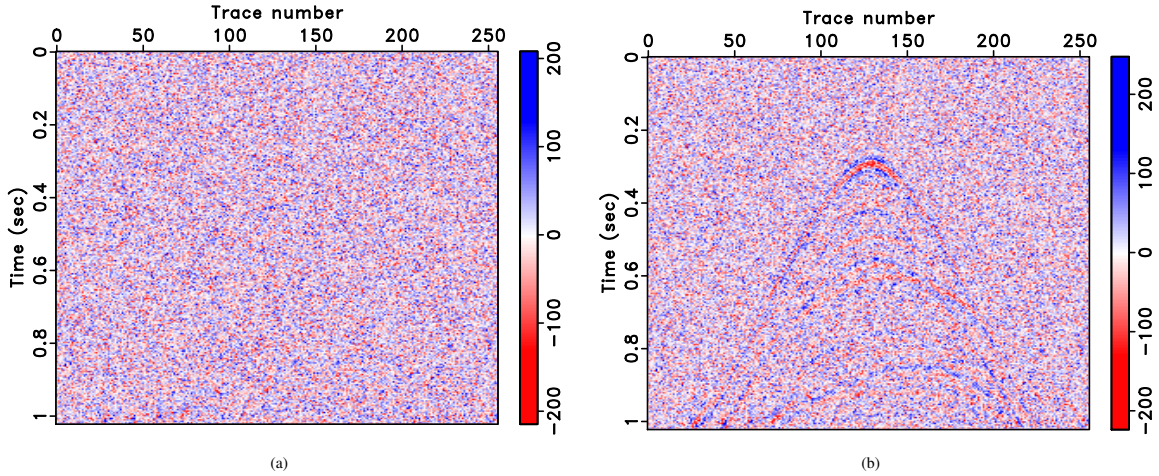

Figure 5: Difference image for white noise: (a) hard thresholding , (b) soft thresholding.

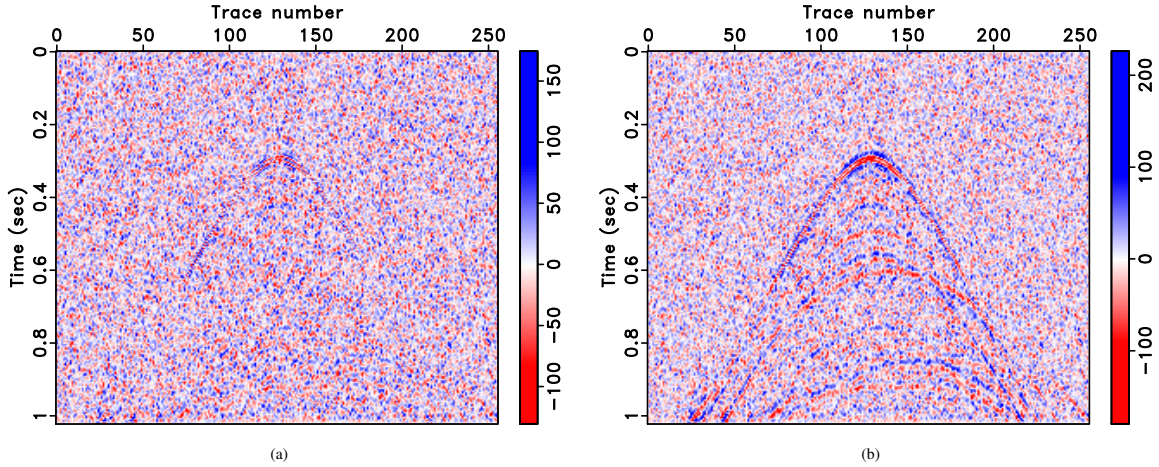

Figure 6: Difference image for colored noise: (a) hard thresholding , (b) soft thresholding.

ACKNOWLEDGMENTS

This work was in part financially supported by the NSERC Discovery Grant 22R81254 and CRD Grant DNOISE 334810-05 of F.J. Herrmann and was carried out as part of the SINBAD project with support, secured through ITF, from the following organizations: BG Group, BP, Chevron, ExxonMobil and Shell.

REFERENCES

Candés, E., L. Demanet, D. Donoho, and L. Ying, 2006, Fast discrete curvelet transforms: Multiscale Modeling and Simulation, **5**, 861–899.

Candés, E., J. Romberg, and T. Tao, 2005, Stable signal recovery from incomplete and inaccurate measurements: Comm. Pure Appl. Math., **59**, 1207–1223.

Daubechies, I., M. Defrise, and C. De Mol, 2004, An iterative thresholding algorithm for linear inverse problems with a sparsity constraints: CPAM, **57**, 1413–1457.

Elad, M., J. L. Starck, P. Querre, and D. L. Donoho, 2005, Simultaneous Cartoon and Texture Image Inpainting using Morphological Component Analysis (MCA): ACHA, **19**, 340–358.

Hennenfent, G., F. J. Herrmann, and R. Neelamani, 2005, Sparseness-constrained seismic deconvolution with Curvelets: Presented at the CSEG National Convention.

Herrmann, F. J. and G. Hennenfent, 2008, Non-parametric seismic data recovery with curvelet frames: Geophysical Journal International, **173**, 233–248.

Lustig, M., D. L. Donoho, and J. M. Pauly, 2007, Sparse MRI: The application of compressed sensing for rapid MR imaging: Magnetic Resonance in Medicine. (In press. `http://www.stanford.edu/~mlustig/SparseMRI.pdf`).

Neelamani, R., A. I. Baumstein, D. G. Gillard, M. T. Hadidi, and W. L. Soroka, 2008, Coherent and random noise attenuation using the curvelet transform: The Leading Edge, **27**, 240–248.